ELSEVIER

Avoiding self-repulsion in density functional description of biased molecular junctions

Roi Baer *, Ester Livshits, Daniel Neuhauser

*Department of Physical Chemistry and The Lise Meitner Minerva-Center for Computational Quantum Chemistry,
The Hebrew University of Jerusalem, Jerusalem 91904, Israel*

Abstract

We examine the effects of self-repulsion on the predictions of charge distribution in biased molecular junctions by the local density functional theory methods. This is done using a functional with explicit long-range exchange term effects [R. Baer, D. Neuhauser, Phys. Rev. Lett. 94 (2005) 043002]. We discuss in detail the new density functional, pointing out some of the remaining difficulties in the theory. We find that in weakly coupled junctions (the typical molecular electronics case) local-density functionals fail to describe correctly the charge distribution in the intermediate bias regime.
© 2006 Elsevier B.V. All rights reserved.

Keywords: Density functional theory; Molecular electronics; Electron correlation

1. Introduction

Self-repulsion is a prevalent problem in density functional theory (DFT), to which various approaches of analysis and solutions have been developed [1–18]. Physically, an electron should not repel itself; however, the Coulomb direct interaction term in DFT has an electron–electron repulsion which does not distinguish between the electrons, so that each electron, in addition to repelling other electrons, repels itself as well. In Hartree–Fock (HF) theory the self-repulsion of an electron is exactly cancelled by the exchange interaction. Such exact cancellation is missing in standard DFT approaches, such as the local-density spin density approximation (LSDA) [19], the generalized gradients approaches [5,20,21] where the exchange is expressed as a local function of the electronic density or the popular hybrid methods [22] where only a small part of explicit exchange is used.

The self-repulsion problem is prevalent in any description of a system with separated parts, be it an ionization problem (where at the final state the electron and the molecule are well separated), electron affinity, or Rydberg state. The problem might be especially acute for theoretical estimates of conductance of molecular junctions, for which many methods relying on DFT have been developed [14,23–31]. In molecular electronics, as the bias changes so does the charge distribution on the bridge and contacts; a correct description of this charge distribution is important for understanding the response (in terms of electric current) to the bias.

Before discussing the remedies to self-repulsion we present the simplest physical ramifications of the phenomena. The problem is clearly seen in systems which contain at least two separate subsystems which are weakly coupled. Such a system could be as simple as two widely spaced hydrogen atoms, or more complicated such as two quantum dots, or a charge transfer complex. We will start with the absolutely simplest system, well-spaced H_2^+ (with large inter-proton distance of, say, 10 a.u.). When the two hydrogen nuclei are well-spaced, the electron is in a symmetric double well, so its density is distributed evenly on

---

* Corresponding author.
  E-mail addresses: roi.baer@huji.ac.il (R. Baer), dxn@chem.ucla.edu (D. Neuhauser).

the two protons. Let us now subject the system to an external bias, i.e., an external electric field. One proton (say the left one) is then biased lower relative to the other. The bias can be quite small, e.g., much less than 1 eV; it only needs to be larger than the weak tunneling coupling for an electron between the two protons. Naturally, the electron under this small bias localizes on the lower potential left proton. We obtain hydrogen atom with a nearby proton: H^+–H. This is a manifestation of a general principle of quantum mechanics: several weakly coupled systems distribute charge in such a way that each has a total charge equaling an integer multiple of the electron charge. This is generally true, as long as the rare tunneling resonances are not operative. This quantization is also related directly to the concept of derivative discontinuities in DFT [3,4]. The ability of approximate electronic structure methods to obey this rule is an important estimate of its robustness. Hartree–Fock theory, for example respects this principle.

DFT, which uses a non-interacting electron description, is expected to obey the integer electron principle as well. However, the standard local approximate functionals of DFT have a troubling feature: in weakly coupled systems they tend to spuriously create resonance conditions in which electrons are much too delocalized. It turns out that in most local functional approximations, as is LSDA there is a continuous leakage of charge, so that, at a bias of 1 eV, say, the density is divided 55% on the lower-biased hydrogen and 45% on the other one. As mentioned above, even at small bias we should see strong charge localization on one of the hydrogen atoms at these distances. The origin of this defect is the presence of the Coulomb repulsion term LSDA which is obviously unphysical here in this one-electron system. The Coulomb electron repulsion is eased a little by transferring some density from the left proton to the right one, and the optimum is reached at 55%. Of course, this is an artifact of LSDA unphysical, since for this 1-electron system there should not be any electron–electron repulsion; the physical value is a single electron on the lower-biased hydrogen. Indeed, solving Schrodinger's equation on a high quality grid shows for the same system that 99.9% of the electronic charge is on the low biased proton while only 0.1% is on the other.

A more formal way to characterize the problem is to note that physically the plot of the excess charge as a function of bias should be almost step-like; when the left hydrogen is biased lower all the density is on it, and for the opposite bias the right hydrogen is charged, and the transition between the two regions will take place in a very narrow voltage range. Density functional theory is formally exact with the correct functional. However, LSDA (and generalized gradients approximation (GGA)) cannot address this since they describe exchange locally. Regular hybrid functionals are able to describe some of this effect, but not completely so that they are insufficient for problems which involve separate systems at large distances, although some efforts have been advocated to solving this problem. There have been several approaches to remedy self-repulsion in DFT based on the self-interaction correction [2] or on exact exchange with no correlation removing.

We have recently proved [9] that a hybrid approach to DFT in which the interaction is divided into a short-range part and a long-range part where the exchange is treated exactly, is a formally exact method. The only unknown in the division is the exact value of the division parameter, but we know a priori that at one value of the parameter the division is exact. In addition, for practical applications, an approximation is needed for the local short-range part, which we treat with an LSDA approach; however, this part by its structure should be well described with local approaches. In this paper we first review in detail the theory of the new functional (which we label "$\gamma = 1$"), including two possible ways to implement it. We then apply it to study the effect of self-repulsion in standard DFT approximations in biased molecular junctions, including especially a prototypical case of a system under bias connected to leads; in our case this will be two metallic spheres acting as leads connected to a smaller sphere representing a molecule under bias.

2. Theory

2.1. The exchange correlation energy

We now describe a new functional which is appropriate for long-range charge transfer so that it is appropriate for describing systems which are weakly coupled, and at the same time keeps a good description of the chemical bonding. This section repeats in greater detail the derivation in Ref. [9].

The starting point is a division of the electron–electron Coulomb repulsion to two part, a shielded and a deshielded one, an idea first proposed by Savin [32], and further developed by Iikura et al. [16]. The deshielded potential is effective only at large distance, and falls off to a constant at short ranges; we use here Yukawa or Gaussian forms:

$$u_\gamma(r) = \begin{cases} \frac{1-e^{-\gamma r}}{r} & \text{Yukawa,} \\ \frac{\text{erf}(\gamma r)}{r} & \text{Gaussian,} \end{cases} \tag{2.1}$$

where γ is a parameter that characterizes the fall-off of the interaction. Other splitting functions are possible, and a recent interesting example is the erfgau function by Toulouse et al. [33], which completely eliminates electron–electron repulsion at short distance. The important feature is that γ is a continuous parameter such that for $\gamma = \infty$ we recover the usual Coulomb interaction in the deshielded part, while any finite positive value of γ is associated with a damped deshielded potential which is finite at $r = 0$ and yields $1/r$ at large distances; for $\gamma = 0$ the electron–electron repulsion vanishes and we are left with a non-interacting system.

Another useful quantity is the shielded potential (the potential complementary to the deshielded, with respect to the Coulomb potential) is

$$y_\gamma(r) = \frac{1}{r} - u_\gamma(r) = \begin{cases} \frac{e^{-\gamma r}}{r} & \text{Yukawa,} \\ \frac{1 - \text{erf}(\gamma r)}{r} & \text{Gaussian,} \end{cases} \quad (2.2)$$

and it falls off rapidly to zero at intermediate and large distances.

We use the new potential in the definition of the total energy, as follows. The full exchange correction for the fully-interacting system (i.e., for electrons that interact with the original Coulombic potential) is written using the adiabatic connection theory [34–36] as an integral [9]:

$$E_{XC}[n] = \int_0^\infty \langle \Psi_{\gamma'} | \hat{W}_{\gamma'} | \Psi_{\gamma'} \rangle \, d\gamma' - E_H[n], \quad (2.3)$$

Ψ_γ refers to the ground-state wavefunction of an interacting system under a Hamiltonian:

$$\hat{H}_\gamma = \hat{T} + \hat{V}_\gamma + \hat{U}_\gamma, \quad (2.4)$$

where $\hat{U}_\gamma$ is a deshielded electron–electron Coulomb potential operator

$$\hat{U}_\gamma = \frac{1}{2} \sum_{i \neq j} u_\gamma(r_{ij}), \quad (2.5)$$

i.e., the electron interact via the deshielded potential, $\hat{T}$ is the kinetic energy of the electrons and $\hat{V}_\gamma$ is a one-body potential which is designed to keep the ground-state density, $n(\mathbf{r})$ fixed as a function of the coupling parameter γ.

The final terms in Eq. (2.3) are the Hartree energy

$$E_H[n] = \frac{1}{2} \iint \frac{n(\mathbf{r})n(\mathbf{r}')}{|\mathbf{r} - \mathbf{r}'|} \, d^3\mathbf{r} \, d^3\mathbf{r}', \quad (2.6)$$

and the two-body term $\hat{W}_\gamma$, which is defined as the derivative of the two-body potential as a function of the coupling parameter, so:

$$\hat{W}_\gamma = \frac{1}{2} \sum_{i \neq j} w_\gamma(r_{ij}), \quad (2.7)$$

where

$$w_\gamma(r) = \frac{du_{\gamma(r)}}{d\gamma}, \quad (2.8)$$

so that for the Yukawa and Gaussian-type potentials, respectively,

$$w_\gamma(r) = \frac{du_\gamma(r)}{d\gamma} = \begin{cases} e^{-\gamma r} & \text{Yukawa,} \\ \frac{2}{\sqrt{\pi}} e^{-(\gamma r)^2} & \text{Gaussian.} \end{cases} \quad (2.9)$$

Eq. (2.3) cannot be solved exactly since the integrand is not generally known. The problem is that for determining the wavefunction, even in a Monte-Carlo approach, one needs to know V_γ, the one-body potential; this potential depends on the integration parameter so that when γ changes the one-body potential needs to change so that the full density is unchanged. We do know however much about the potential and the wavefunction at the two extrema of γ. For $\gamma = \infty$, i.e., no deshielding, the one-body potential is the original electron–nuclear potential, and the wavefunction is the complete many-body interacting one. For $\gamma = 0$,

i.e., no interaction, the one-body potential is exactly the Sham potential (which by definition is the potential needed to reproduce for non-interacting system the original density) and the wavefunction is a Slater-determinant (assuming no degeneracies) of non-interacting orbitals. This information gives us a good starting point for approximations.

The first approximation uses information from just one value, $\gamma = 0$, i.e., assumes that the wavefunction does not depend on γ' and replaces $\Psi_{\gamma'}$ by Ψ_0. As is easy to see this yields the Hartree exchange approximation for E_{XC}. The next level uses information from both $\gamma = 0$ and $\gamma = \infty$, by approximating that

$$\Psi_{\gamma'} \simeq \begin{cases} \Psi_0 & \gamma' < \gamma, \\ \Psi_\infty & \gamma' > \gamma, \end{cases} \quad (2.10)$$

i.e., replacing the wavefunction by the end values; here γ is a parameter which designates the division point. (As proved in Ref. [9] and explained below, there is a definite but unknown value of γ where the approximation (2.10) gives an accurate value of the exchange-correlation energy.)

Formally the approximation (2.10), when inserted in the adiabatic connection formula (Eq. (2.3)), gives:

$$E_{XC}[n] \cong \left\langle \Psi_0 \left| \int_0^\gamma \hat{W}_{\gamma'} \, d\gamma' \right| \Psi_0 \right\rangle$$
$$+ \left\langle \Psi_\infty \left| \int_\gamma^\infty \hat{W}_{\gamma'} \, d\gamma' \right| \Psi_\infty \right\rangle - E_H[n]. \quad (2.11)$$

In Ref. [9] we showed that for any system, there exists a value of the shielding parameter $\gamma[n]$ that renders Eq. (2.11) *exact*:

$$E_{XC}[n] = \langle \Psi_0 | \hat{U}_\gamma | \Psi_0 \rangle + \langle \Psi_\infty | \hat{Y}_\gamma | \Psi_\infty \rangle - E_H[n], \quad (2.12)$$

where we introduce the operator for the screened part of the Coulomb potential

$$\hat{Y}_\gamma = \frac{1}{2} \sum_{i \neq j} y_\gamma(r_{ij}). \quad (2.13)$$

We can pull out of E_{XC} an exact exchange part with respect to the interaction u_γ. This gives:

$$E_{XC}[n] = E_X^{u_\gamma}[n] + \langle \Psi_\infty | \hat{Y}_\gamma | \Psi_\infty \rangle$$
$$- \frac{1}{2} \int n(\mathbf{r})n(\mathbf{r}') y_\gamma(|\mathbf{r} - \mathbf{r}'|) \, d^3r \, d^3r', \quad (2.14)$$

where $E_X^{u_\gamma}[n]$ is an explicit exchange defined by

$$E_X^{u_\gamma}[n] = -\frac{1}{2} \iint P(\mathbf{r}, \mathbf{r}')^2 u_\gamma(|\mathbf{r} - \mathbf{r}'|) \, d^3\mathbf{r} \, d^3r', \quad (2.15)$$

where $P(\mathbf{r}, \mathbf{r}')$ is the non-interacting (Kohn–Sham) density matrix. Eq. (2.14) can be written in terms of the exchange correlation hole $n_{XC}(\mathbf{r}, \mathbf{r}') = n(\mathbf{r}')[g_{XC}(\mathbf{r}, \mathbf{r}') - 1]$ where $g_{XC}(\mathbf{r}, \mathbf{r}')$ is the pair correlation function:

$$E_{XC}[n] = E_X^{u_\gamma}[n] + \frac{1}{2} \int n(\mathbf{r}) n_{XC}(\mathbf{r}, \mathbf{r}') y_\gamma(|\mathbf{r} - \mathbf{r}'|) \, d^3r \, d^3r'. \quad (2.16)$$

Eq. (2.16) should be compared to the well-known expression for the XC energy, using the averaged exchange-correlation hole [1]:

$$E_{XC}[n] = \frac{1}{2} \iint \frac{n(\mathbf{r})\bar{n}_{XC}(\mathbf{r},\mathbf{r}')}{|\mathbf{r}-\mathbf{r}'|} \, d^3r \, d^3r'. \tag{2.17}$$

Note that the XC hole in Eq. (2.16) is that of the system, while in Eq. (2.17) appears an adiabatically averaged XC hole:

$$\bar{n}_{XC}(\mathbf{r},\mathbf{r}') = \int_0^1 n_{XC}^\lambda(\mathbf{r},\mathbf{r}') \, d\lambda, \tag{2.18}$$

where n_{XC}^λ is the XC hole of a system of electrons having of density $n(\mathbf{r})$ but interacting via the potential $v_\lambda(r_{12}) = \lambda/r_{12}$. Eq. (2.16) has the property of isolating an explicit exchange term with respect to the long-range interaction. This term by itself formally removes of the self-repulsion in the resulting functional. Of course, one disadvantage of Eq. (2.16) is that there appears a new functional $\gamma[n]$ which in general is unknown.

2.2. A practical size-consistent approach to γ

One approach to using the theory for obtaining an approximate DFT is to take γ equal to some constant (e.g., $\gamma = 1$ a.u.) for all systems. This is complemented by an appropriate correlation energy. While this is a drastic approximation, it has the benefit of being size consistent. As shown below, the results based on this approximation are not overly sensitive to the value of the constant chosen. For the Yukawa parameter we generally choose $\gamma = 1a_0^{-1}$. The theoretical drawback of this method is that it is not exact in any analytical known limit (such as the homogeneous electron gas). We discuss below an alternative approach which does not suffer from this drawback.

In order to use this approximation, we further assume that a local approximation is valid for E_{XC}^γ in (2.16)

$$E_{XC}^\gamma \cong \int \varepsilon_{XC}^\gamma(n(\mathbf{r}))n(\mathbf{r}) \, d^3\mathbf{r}. \tag{2.19}$$

Here, $\varepsilon_{XC}^\gamma(n(\mathbf{r}))$ is computed using the partitioning:

$$\varepsilon_{XC}^\gamma \equiv \varepsilon_X^{\gamma} + \varepsilon_C^\gamma. \tag{2.20}$$

The first part is the exchange energy of a homogenous electron gas (HEG) whereby the particles are interacting via a screened (shielded) Coulomb potential. It is given by

$$\varepsilon_X^{\gamma}(n) = -\frac{3k_F}{4\pi} H\left(\frac{\gamma}{k_F}\right), \tag{2.21}$$

where k_F is the Fermi momentum of the HEG, $k_F = (3\pi^2 n)^{1/3}$ and [37]

$$H(q) = 1 - \frac{q^2}{6} - \frac{4q}{3}\tan^{-1}\left(\frac{2}{q}\right) + \frac{q^2}{24}(12+q^2)$$
$$\times \ln\left(\frac{4}{q^2+1}\right) \quad \text{(Yukawa)}, \tag{2.22}$$

or [38]

$$H(q) = 1 - \frac{4\sqrt{\pi}}{3}q\,\mathrm{erf}\left(\frac{1}{q}\right)$$
$$+ \frac{2}{3}q^2\left\{1 - (q^2-2)\left[1 - e^{-\frac{1}{q^2}}\right]\right\} \quad \text{(Gaussian)}. \tag{2.23}$$

A first approximation for the correlation energy can be computed by adopting Eq. (2.16) for the HEG:

$$\varepsilon_C^\gamma(n) = \frac{n}{2}\int_0^\infty g_C^{\mathrm{hom}}(n,x)y_\gamma(x)4\pi x^2 \, dx. \tag{2.24}$$

The treatment of polarized gases is straightforward. Since exchange exists only between particles of like spins, the exchange energy must abide to the rule [39]:

$$E_X[n_\uparrow, n_\downarrow] = (E_X[2n_\uparrow, 0] + E_X[0, 2n_\downarrow])/2. \tag{2.25}$$

The correlation energy can be handled by using the "polarized" pair correlation function $g_C(r_s, \zeta, k_F r)$ for the HEG. Here $r_s = (3/4\pi n)^{1/3}$ is the density parameter, $\zeta = (n_\uparrow - n_\downarrow)/n$ is the spin polarization and $k_F = (3\pi^2 n)^{1/3}$ is the Fermi wave-vector. This function has been thoroughly parameterized recently, based on accurate Monte Carlo calculations for the fully polarized and unpolarized HEG and on various known sum rules and exact conditions [40,41]. We plot in Fig. 1 the ratio

$$\eta = \varepsilon_C^\gamma/\varepsilon_C^{\mathrm{LSDA}}, \tag{2.26}$$

where $\varepsilon_C^{\mathrm{LSDA}}$ is the LSDA correlation energy (i.e., the correlation energy of a HEG). For valence electrons the density parameter is typically $1 < r_s < 5$. In this range (for $\zeta = 0$) η is close to but usually less than 1. Thus, the correlation energy of the on-homogeneous finite system is somewhat weakened. It is also seen that in the high density limit (when $r_s \to 0$) η converges to 2, while $\eta \to 0$ for low densities.

The η function for the Gaussian partitioning is shown in Fig. 2. We find that the Yukawa η curve at $\gamma = 1a_0^{-1}$ is similar in shape to the Gaussian η curve at $\gamma = 0.6a_0^{-1}$.
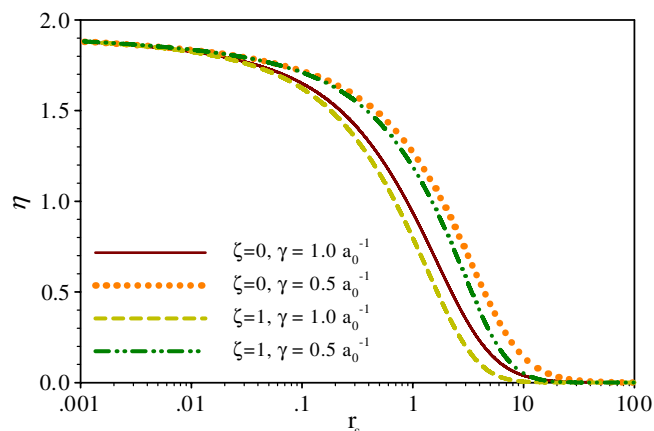

Fig. 1. The ratio of ε_C^γ to the LSDA correlation energy (as parameterized in Ref. [45]) for the Yukawa partitioning.
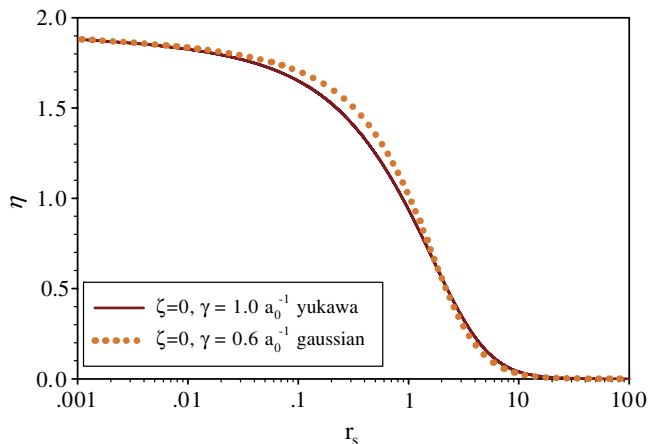
Fig. 2. The ratio η for Gaussian and Yukawa partitioning of the interaction.

2.3. An approach to γ consistent with the HEG

Although the method discussed in Section 2.2 is size-consistent, it suffers from the fact that it does not reproduce correct results in the HEG limit. In fact, for the HEG we should have $\varepsilon_C^{\gamma} = \varepsilon_C^{\text{LSDA}}$. Thus we can determine the exact $\gamma^{\text{HEG}}(r_s)$ from the equation

$$\eta\big(\gamma^{\text{HEG}}(r_s, \zeta)\big) = 1. \tag{2.27}$$

The function γ^{HEG} can be computed to high degree of accuracy using the Monte-Carlo based parameterization of the pair correlation function [41]. We plot γ^{HEG} in Fig. 3. A simple functional form can be used to approximate γ^{HEG}, in a region of $0.01 < r_s < 20$:

$$\gamma^{\text{HEG}}(r_s) = \frac{1}{a r_s^c (1 + b^2 r_s^d)}. \tag{2.28}$$

The four parameters, giving useful accuracy are shown in Table 1, as function of the case.
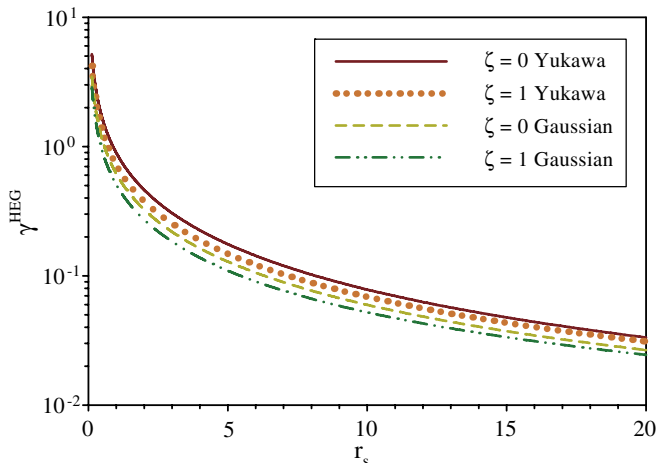

Fig. 3. γ^{HEG} as a function of the density parameter r_s for the unpolarized and fully polarized electron gas.

Table 1
The parameters for use in Eq. (2.28)

	a	b	c	d
Yuk, $\zeta = 0$	0.9520	0.4281	0.7887	0.7770
Yuk, $\zeta = 1$	1.1121	0.5103	0.7824	0.5823
Gau, $\zeta = 0$	1.6478	0.4576	0.7821	0.5509
Gau, $\zeta = 1$	1.6730	0.4361	0.7847	0.5867

For a non-homogeneous system we need to define functional $\gamma[r_s, \zeta]$ such that if $r_s(\mathbf{r}) = r_s^0$ and $\zeta(\mathbf{r}) = \zeta^0$ then $\gamma[r_s, \zeta] = \gamma^{\text{HEG}}(r_s^0, \zeta^0)$. The problem is that there are infinitely many ways to do this. For example, one can take a "local density" average:

$$\gamma[n_\uparrow, n_\downarrow] = \frac{\int \gamma^{\text{HEG}}(r_s(\mathbf{r}), \zeta(\mathbf{r})) n(\mathbf{r}) \, d^3 r}{\int n(\mathbf{r}) \, d^3 r}. \tag{2.29}$$

Another possibility is to use $\gamma[n_\uparrow, n_\downarrow] = \gamma^{\text{HEG}}(\bar{r}_s, \bar{\zeta})$ where $\bar{r}_s$ and $\bar{\zeta}$ are suitably averaged density and spin polarization parameters. Unfortunately, there are infinitely many different ways to determine $\bar{r}_s$ (or $\bar{\zeta}$) for a non-homogeneous system, which in the case of a constant n will give the HEG density parameter. From the Thomas–Fermi–Dirac theory, the non-interacting kinetic energy per particle in HEG is $t_S^{\text{HEG}} = 3k_F^2/20$ and the exchange energy per particle is (in atomic units) $\varepsilon_X^{\text{HEG}} = -3k_F/4\pi$, where $k_F = \alpha/r_s$ is the Fermi wave-vector and $\alpha \equiv (9\pi/4)^{1/3}$. Using these relations, one can define various functionals for the "average density parameter" for non-homogeneous systems as follows:

$$\bar{r}_s^{(1)} = -\frac{3\alpha N_e}{4\pi E_X} \quad \text{or} \quad \bar{r}_s^{(2)} = -\frac{\pi\alpha}{5}\left(\frac{E_X}{T_s}\right). \tag{2.30}$$

For the HEG both $\bar{r}_s^{(1)}$ and $\bar{r}_s^{(2)}$ give the same correct value of r_s. However, for non-uniform systems they can lead to significantly different estimates of the average density parameter. For example, using the valence electron density of N_2 $\bar{r}_s^{(1)} \approx 1.0$ while $\bar{r}_s^{(2)} \approx 0.4$ (note that when the 1s core electrons are included, their high kinetic energy causes $r_s^{(2)}$ to drop to extremely low values, around 0.1). With these two estimates for we can create for N_2 practically any value we want for $\bar{r}_s$, for example taking $\bar{r}_s^{(3)} \equiv (\bar{r}_s^{(2)})^2 / \bar{r}_s^{(1)}$, yields using the above numbers $\bar{r}_s^{(3)} = 2.5$. Clearly, additional physical insight must be sought before a proper theory for γ can be established. Since we do not have a complete theory at present we will be using the constant γ approach of Section 2.2 in the application part of the paper.

3. Results

In this section we give several applications the functional. Since the functional includes an explicit exchange term it uses the total one-body density matrix rather than the local density alone, so it needs to be applied and checked carefully. The simplest approach is to minimize the total energy as a functional of the occupied orbitals, similar to the Hartree–Fock theory. This minimizing procedure gives the following orbital equations:

$$-\frac{1}{2}\nabla^2\psi_i + [v_{\text{ext}}(\mathbf{r}) + v_{\text{H}}(\mathbf{r}) + v_{\text{XC}}^{\text{local}}(\mathbf{r}) + \hat{K}]\psi_i = \varepsilon_i\psi_i, \qquad (3.1)$$

where $\psi_i(\mathbf{r})$ are the Kohn–Sham orbitals, ε_i the orbital energies and v_{ext} the external potential on the electrons. This potential also includes in some of the calculations below a non-local pseudopotential. $v_{\text{H}}(\mathbf{r}) = \int n(\mathbf{r}')\,\mathrm{d}^3r'/|\mathbf{r}-\mathbf{r}'|$ is the Hartree potential and

$$v_{\text{XC}}^{\text{local}}(\mathbf{r}) = \varepsilon_{\text{XC}}^{\gamma}(n(\mathbf{r})) + n(\mathbf{r})\varepsilon_{\text{XC}}^{\gamma\prime}(n(\mathbf{r})). \qquad (3.2)$$

The operator $\hat{K}$ in Eq. (3.1) is the explicit exchange operator, dependent on the Kohn–Sham orbitals, in an identical way the Hartree–Fock exchange depends on the Hartree–Fock orbitals.

Since in our application the potential is non-local, we need to get a local form. This is done by constructing the *effective potential*, defined as

$$v_{\text{eff}}(\mathbf{r}) = \frac{\sum_{i=1}^{N_e}\psi_i^*(\mathbf{r})(\varepsilon_i + \frac{1}{2}\nabla^2)\psi_i(\mathbf{r})}{n(\mathbf{r})}. \qquad (3.3)$$

For a regular local Kohn–Sham potential, the effective potential equals the local potential as is evident from Eqs. (3.1)–(3.3).
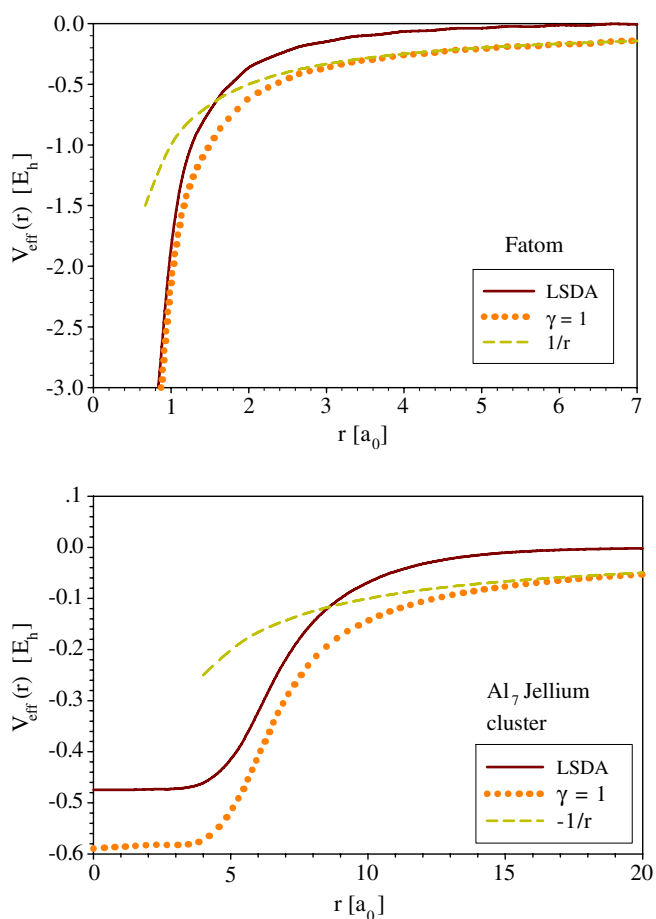

Fig. 4. The effective potential according to the "$\gamma = 1$" theory, the LSDA and the $-1/r$ potential. Top: in fluorine atom; bottom: spherical jellium model at densities of aluminum.

3.1. Effective potential and polarizability

Fig. 4 shows the effective potential of two neutral system, an fluorine atom and a spherical metallic cluster (modeled by as a jellium sphere with density parameters $r_s = 2.1$). The exact DFT effective potential of a neutral system should asymptotically be [42]

$$\lim_{r\to\infty} v_{\text{eff}}(\mathbf{r}) = \frac{-1}{r}. \qquad (3.4)$$

Physically, this is due to the fact that when an electron is pulled away from a neutral system it "leaves behind" a positively charged ion $q = +1$ to which it is then attracted. It is well known that the effective potentials of the LSDA do not exhibit this feature, as verified in Fig. 4. This fact causes some problems with the general applicability of LSDA. For example, the Rydberg series is not correctly reproduced by the virtual energies. This has also ramifications in the use of ALSDA. On the other hand, the effective potential arising from the new functional exhibits this desirable property.

A correct effective potential leads to qualitatively correct polarizability. In Ref. [9] we showed that the functional leads to the improved prediction of polarizability for a chain of H_2 molecules as a function of it length. While LSDA overestimates the polarizability as being nearly linear with the length of the chain, the $\gamma = 1$ theory shows, in accordance with Hartree–Fock and MP2 calculations that the polarizability levels off beyond about 5 oligomers.

3.2. Systems under bias: two metallic clusters

Next we finally come back to the issues posed in the beginning of the paper, namely charge quantization for two separate systems under bias.

The problem with LSDA, explained earlier for H_2 appears for other systems too. Whenever a system is made of two or more weakly coupled subparts then, at a large distance, the ground-state should have an integer number of electrons, but LSDA (as well as other local functionals) optimizes the Coulomb energy by having non-physical partial charges on the weakly coupled subparts.

The same features are qualitatively important even in larger system. Specifically, we simulate two nanometer sized gold or silver clusters, using a spherical jellium model (Fig. 5). Two spheres are set a distance of $R = 28a_0$. The positive charge density in each ball is of a smoothed Fermi–Dirac form, i.e.,

$$n(r) = \frac{n_0}{1 + \mathrm{e}^{(r-r_0)/\sigma_0}}. \qquad (3.5)$$

The jellium bulk density n_0 corresponds to a Seitz parameter of $r_s = 3a_0$, similar to the positive charge density of gold or silver. The radius of each ball is $r_0 = 6a_0$ and the width of the jellium edge is $\sigma = 0.4a_0$. With this density the system is a rough model for small gold or silver clusters.
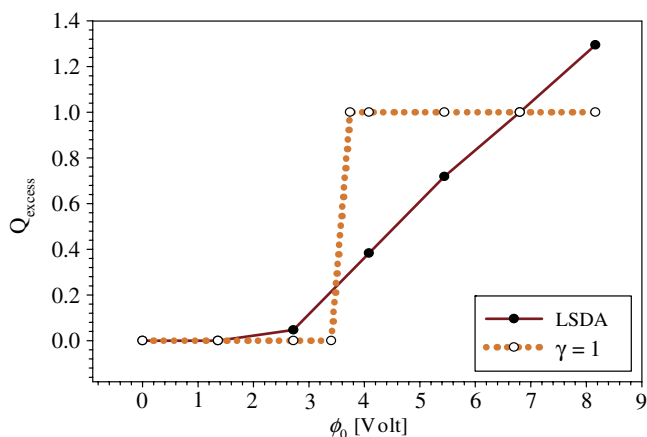
Fig. 5. The excess charge on the right cluster as a function of the bias ϕ_0. Shown, the result of the LSDA and the $\gamma = 1$ calculations.

The overall positive charge on each sphere is $20e$, so we have used 40 electrons in this neutral system.

To the pair of spheres we add an external electric potential

$$\phi(z) = \frac{1}{2}\phi_0 \sin\frac{2\pi z}{L}, \qquad (3.6)$$

which biases one sphere with respect to the other. For technical reasons (preserving periodic boundary conditions) we use a periodic bias, with L the simulation box length and the parameter ϕ_0 represents the bias (Fig. 5). The external potential $\phi(z)$ which is positive in the right ball, decreases within a transition region between the balls, and is a negative within the left ball. The potential energy due to the bias voltage is $-e\phi(z)$. Thus, electrons are attracted to the left well.

Since the spheres are so well separated, the qualitative features of this charge system will be identical to that of the stretched H_2 double-well system: at small bias there should be no charge transfer and once the bias exceeds a threshold, there is a full transfer of an electron. The critical bias voltage equals:

$$\phi_c \approx IP - EA - \frac{1}{R - 2r_0}, \qquad (3.7)$$

where IP is the ionization potential and EA the electron affinity of a single sphere. $R - 2r_0$ is the distance between the surfaces of the spheres and is approximately the distance between the electron and the hole it leaves behind. Fig. 5 shows that LSDA misses this qualitative feature, while the new functional obtains it. Note that the step-function behavior occurs at the bias $\phi_c = 3.7$ V. This number should compared with the estimate of Eq. (3.7). This can be done by two independent ways of estimating IP − EA of a single sphere:

$$\begin{aligned} \Delta SCF: \quad & IP = E_N - E_{N-1} \quad EA = E_{N+1} - E_N, \\ HOMO: \quad & IP = -\varepsilon_N \quad EA = -\varepsilon_{N+1}. \end{aligned} \qquad (3.8)$$

In the first method we use the ground-state total energies of the neutral (E_N), the cation (E_{N-1}) and the anion (E_{N+1})

Table 2
$\gamma = 1$ Estimates of the critical bias (all quantities in volts)

ΔSCF			HOMO		
IP	EA	ϕ_c	IP	EA	ϕ_c
5.6	0.5	3.5	6.2	0.8	3.7

Shown, estimates of IP, EA and ϕ_c (Eq. (3.7)) computed using the ΔSCF and $\Delta\varepsilon_H$ methods of Eq. (3.8).

clusters while in the second method we use the HOMO energies of the neutral ε_N and the anion ε_{N+1}, based on the theorem in (exact) DFT that the HOMO energy is equal to the electron removal energy [4,42]. The results for the $\gamma = 1$ functional are shown in Table 2, where the estimated critical bias is compatible with the value found for the two sphere system (3.7 V).

Note that due to the small size of the sphere, LSDA predicts that an anion is unbound. This leads to unreliable calculations of the electron affinity and ϕ_c is difficult to estimate. If one takes EA = 0 for the LSDA, one obtains $\phi_c = 3.5$ V in the ΔSCF method and $\phi_c = 4.1$ V in the HOMO method.

3.3. Model for a molecular-scale junction under bias

We now turn to consider the biased molecular-scale junction. Our model junction is composed of two spherical jellium clusters with the density of gold and diameter of $12a_0$, serving the role of leads, and a sphere of smaller size, playing the role of a bridge situated in between the leads. The centers of the two spherical leads are $28a_0$ apart so that their average edges are at a minimal distance of $16a_0$. The small spherical conductor contains only 2 electrons, and is situated in the middle.

On this junction we applied an external potential using a sin-type bias Eq. (3.6) (the form of this potential is shown in Fig. 8) . The calculated charge transfer vs. bias voltage is shown in Fig. 6. Because of the presence of the bridge, it is not a step function but still shows a sharp transition: a weak slope $dQ/d\phi_0$ is maintained up to a critical voltage
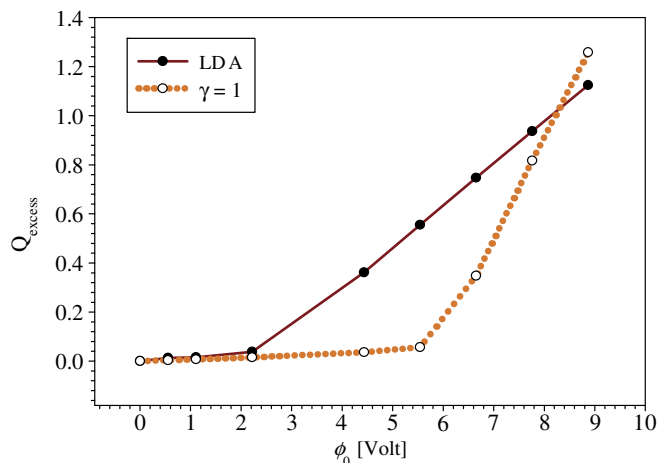

Fig. 6. The excess charge on the right lead as a function of the bias between the two leads. Shown, LSDA and $\gamma = 1$ predictions.
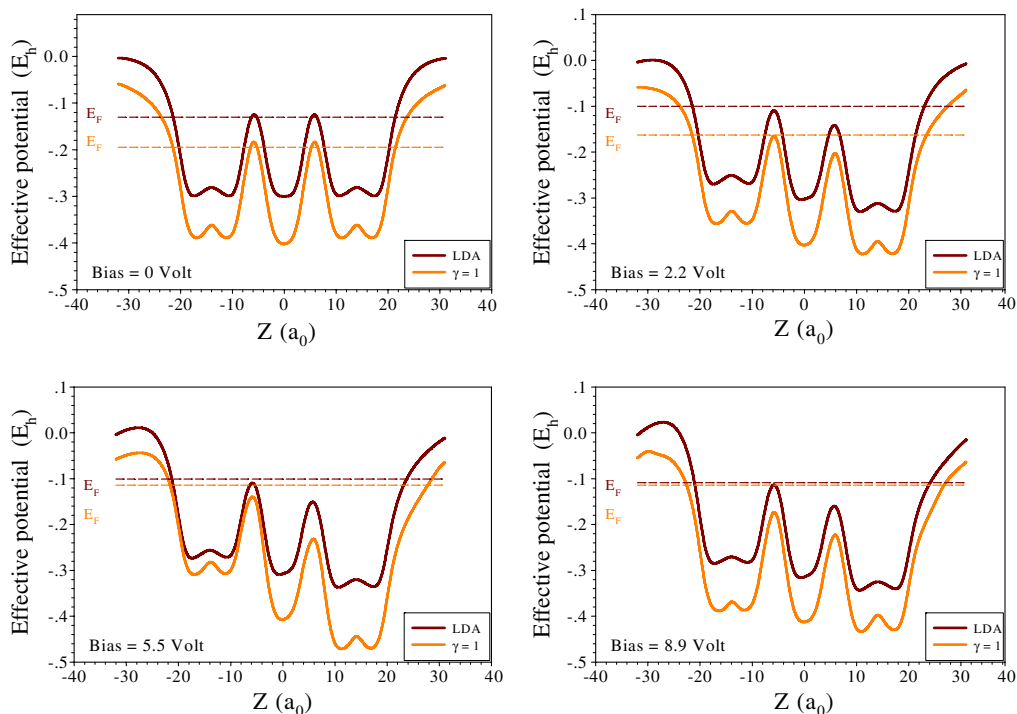
Fig. 7. The effective potential for the biased junction: results for an LSDA and a $\gamma = 1$ density functional calculations are shown, for various external bias potential. Fermi level is also shown for both cases.

of about 5.6 V, followed by a sharp linear increase thereafter. The reason for this more continuous behavior is that the lead-bridge coupling is not very weak, so charge can delocalize over the bridge. It is evident that he LSDA and $\gamma = 1$ functionals have vastly different predictions at intermediate biases of several volts.

Next, the effective potential, defined in (3.3), was studied, shown in Fig. 7 as a function of the external bias. At zero bias and also for a low (< 2.2 V) and large (>5.5 V) biases the qualitative features of the potentials are similar for the two functionals – minima for the leads (i.e., the large balls) and at the middle ball, and the value of the minima decrease
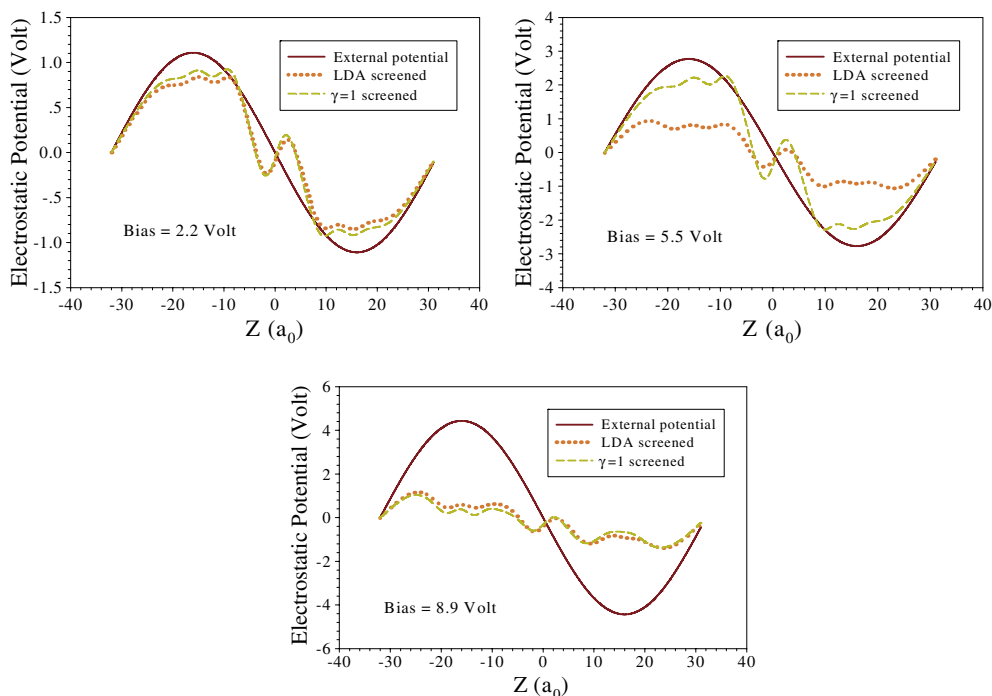

Fig. 8. The electrostatic potentials: at low (high) bias the screening is weak (very strong) and the two theories agree. At intermediate bias the two theories give different electrostatic potentials.

approximately linearly from left to right, with similar slope, i.e., similar electric field. However, for a large (but not too large) bias, at 5.5 eV, a new behavior occurs. The slope is now much larger; the reason is that there is charge transfer between the two spheres in the LSDA approach, which masks the external field, but in the new functional, the electron is not yet transferred, as Fig. 6 shows.

Finally, an important quantity for conductance calculations is the total electrostatic potential:

$$v_{es}(\mathbf{r}) = v_H(\mathbf{r}) + v_{ext}(\mathbf{r}). \tag{3.9}$$

Note that this potential is formally different from the effective potential, although it refers to a qualitatively similar aspect.

Fig. 8 shows the electrostatic potential for the junction system. At the lower voltage (2.2 V) the external potential is not screened much, while the very high voltage (8.9 V) there is very strong screening due to charge transfer seen in Fig. 6. The electrostatic potential across the bridge is thus quite flat. The most interesting result is for the high (but not very high) voltage, 5.5 V, where the two theories differ considerably in the prediction: in LSDA considerable charge transfer occurs at 5.5 V, so there is strong screening, while in $\gamma = 1$ theory, the screening is much less.

4. Summary

We have presented approaches to a DFT that avoids long-range self-repulsion. Our method is dependent on a functional $\gamma[n]$ and a correlation energy functional ε_C^γ. We have examined approximations for both these functionals, based on the HEG. One approximation took $\gamma[n]$ to be a constant independent of n. A correlation energy functional was developed based on the exact theory. Another approximation was to take the correlation energy of the HEG as in usual LSDA or GGA but base the γ functional on the HEG. Here we pointed out difficulties in mapping the non-homogeneous system with the homogeneous one. Our conclusion is that at present there is not enough physical insight on which to base the second approach and more work is needed in that direction.

Using the first approximation, where γ is taken as constant, we studied the charge distribution and effective (Kohn–Sham) potentials in biased molecular-scale junctions. We find that in intermediate biases (of a few volts) the charge distribution predicted by LSDA may be incorrect due to the self-repulsion effect.

The next steps for potential applications include studying conductance using the new theory in a time-dependent DFT framework [26,28,43]. An incorrect description of the charge distribution will necessarily lead to errors in conductance calculations, an issue discussed recently [9,14]. The application of a similar theory to compute excitation energies [44] has shown promising results to systems where long-range charge transfer is important.

References

[1] O. Gunnarsson, M. Jonson, B.I. Lundqvist, Phys. Rev. B 20 (1979) 3136.
[2] J.P. Perdew, A. Zunger, Phys. Rev. B 23 (1981) 5048.
[3] J.P. Perdew, R.G. Parr, M. Levy, J.L. Balduz, Phys. Rev. Lett. 49 (1982) 1691.
[4] J.P. Perdew, M. Levy, Phys. Rev. Lett. 51 (1983) 1884.
[5] A.D. Becke, Phys. Rev. A 38 (1988) 3098.
[6] S.J.A. van Gisbergen, P.R.T. Schipper, O.V. Gritsenko, E.J. Baerends, J.G. Snijders, B. Champagne, B. Kirtman, Phys. Rev. Lett. 83 (1999) 694.
[7] P. Mori-Sanchez, Q. Wu, W. Yang, J. Chem. Phys. 119 (2003) 11001.
[8] S. Kummel, L. Kronik, J.P. Perdew, Phys. Rev. Lett. 93 (2004) 213002.
[9] R. Baer, D. Neuhauser, Phys. Rev. Lett. 94 (2005) 043002.
[10] R.M. Dreizler, E.K.U. Gross, Density Functional Theory: An Approach to the Quantum Many Body Problem, Springer, Berlin, 1990.
[11] R.G. Parr, W. Yang, Density Functional Theory of Atoms and Molecules, Oxford University Press, Oxford, 1989.
[12] A. Gorling, J. Chem. Phys. 123 (2005).
[13] A. Dreuw, J.L. Weisman, M. Head-Gordon, J. Chem. Phys. 119 (2003) 2943.
[14] C. Toher, A. Filippetti, S. Sanvito, K. Burke, Phys. Rev. Lett. 95 (2005).
[15] Q. Wu, T. Van Voorhis, Phys. Rev. A 72 (2005) 024502.
[16] H. Iikura, T. Tsuneda, T. Yanai, K. Hirao, J. Chem. Phys. 115 (2001) 3540.
[17] T. Yanai, D.P. Tew, N.C. Handy, Chem. Phys. Lett. 393 (2004) 51.
[18] M.J.G. Peach, T. Helgaker, P. Salek, T.W. Keal, O.B. Lutnaes, D.J. Tozer, N.C. Handy, Phys. Chem. Chem. Phys. 8 (2005) 558.
[19] A. Zangwill, P. Soven, Phys. Rev. A 21 (1980) 1561.
[20] D.C. Langreth, M.J. Mehl, Phys. Rev. B 28 (1983) 1809.
[21] J.P. Perdew, J.A. Chevary, S.H. Vosko, K.A. Jackson, M.R. Pederson, D.J. Singh, C. Fiolhais, Phys. Rev. B 46 (1992) 6671.
[22] A.D. Becke, J. Chem. Phys. 98 (1993) 1372.
[23] M. Di Ventra, S.T. Pantelides, N.D. Lang, Phys. Rev. Lett. 84 (2000) 979.
[24] Y.Q. Xue, S. Datta, M.A. Ratner, Chem. Phys. 281 (2002) 151.
[25] A. Nitzan, M.A. Ratner, Science 300 (2003) 1384.
[26] R. Baer, D. Neuhauser, Int. J. Quant. Chem. 91 (2003) 524.
[27] F. Remacle, R.D. Levine, Chem. Phys. Lett. 383 (2004) 537.
[28] R. Baer, T. Seideman, S. Ilani, D. Neuhauser, J. Chem. Phys. 120 (2004) 3387.
[29] O. Hod, E. Rabani, R. Baer, Acc. Chem. Res. 39 (2006) 109.
[30] N. Sai, M. Zwolak, G. Vignale, M. Di Ventra, Phys. Rev. Lett. 94 (2005) 186810.
[31] A. Nitzan, M. Galperin, G.L. Ingold, H. Grabert, J. Chem. Phys. 117 (2002) 10837.
[32] A. Savin, in: D.P. Chong (Ed.), Recent Advances in Density Functional Methods Part I, World Scientific, Singapore, 1995, p. 129.
[33] J. Toulouse, F. Colonna, A. Savin, Phys. Rev. A 70 (2004).
[34] D.C. Langreth, J.P. Perdew, Sol. Stat. Commun. 17 (1975) 1425.
[35] O. Gunnarsson, B.I. Lundqvist, Phys. Rev. B 13 (1976) 4274.
[36] W. Yang, J. Chem. Phys. 109 (1998) 10107.
[37] J.E. Robinson, F. Bassani, R.S. Knox, J.R. Schreiffer, Phys. Rev. Lett. 9 (1962) 215.

[38] J. Toulouse, A. Savin, H.J. Flad, Int. J. Quant. Chem. 100 (2004) 1047.
[39] G.L. Oliver, J.P. Perdew, Phys. Rev. A 20 (1979) 397.
[40] P. Gori-Giorgi, J.P. Perdew, Phys. Rev. B 6415 (2001).
[41] P. Gori-Giorgi, J.P. Perdew, Phys. Rev. B 66 (2002) 165118.
[42] U. von-Barth, C.-O. Almbladh, Phys. Rev. B 31 (1985) 3231.
[43] S. Kurth, G. Stefanucci, C.O. Almbladh, A. Rubio, E.K.U. Gross, Phys. Rev. B 72 (2005) 035308.
[44] Y. Tawada, T. Tsuneda, S. Yanagisawa, T. Yanai, K. Hirao, J. Chem. Phys. 120 (2004) 8425.
[45] J.P. Perdew, Y. Wang, Phys. Rev. B 45 (1992) 13244.